*Earthquake Engineering, Tenth World Conference © 1992 Balkema, Rotterdam. ISBN 90 5410 060 5*

# Dynamic buckling analysis for cylindrical shell due to random excitation

K. Fujita & T. Ito
*Takasago R&D Center, Mitsubishi Heavy Industries, Ltd, Hyogo, Japan*

K. Baba & M. Ochi
*SI 2nd Center, Mitsubishi Heavy Industries, Ltd, Kobe, Hyogo, Japan*

K. Nagata
*Kobe Shipyard and Machinery Works, Mitsubishi Heavy Industries, Ltd, Hyogo, Japan*

ABSTRACT: The containment vessel of a nuclear power plant, the LMFBR reactor vessel and a tall cylindrical tower are thin cylindrical shell structures with large diameter. Therefore, development of an evaluation technology for dynamic buckling for these structures due to wind or seismic loading is becoming very important. Some research works are found recently, but the analysis generally needs unpractical huge CPU time. The development and the utility of a practical dynamic buckling analysis code using FEM, in which lumped masses and initial imperfection etc. can be taken into account, are reported here.

## 1. INTRODUCTION

Various large cylindrical structures such as a containment vessel, a reactor vessel and a LNG tank can be found in a nuclear power plant or a chemical plant, etc., moreover tall cylindrical towers are also found under construction. These large cylindrical structures tend to become larger in diameter and thinner, therefore, the evaluation on the dynamic buckling due to wind forces or seismic excitation will become more and more important. As for the evaluation on the dynamic buckling for these thin cylindrical structures, several research papers can be found recently. However, some of those technology take unpractical huge CPU time, then it can be said that the practical evaluation methodology is still under development. Yamaki (1984), Tani (1985) and Chiba (1988) studied the dynamic instability of a cylindrical vessel due to horizontal excitation experimentally and analytically in addition to the relationship between the natural frequency and the static force. Combescure (1987) conducted the static and dynamic buckling analysis for a cylindrical vessel using pseudo axisymmetric elements "COMU" and compared to the experimental values. Liu, et al. (1989) studied the dynamic instability introducing the idea of parametric excitation, and obtained a good agreement with the experimental values conducted by Chiba, et al. (1988).

The authors (1990a, 1990b, 1991) have been investigating the dynamic buckling behavior experimentally using cylindrical shells with various dimensions.

In this study, the development and the utility of a practical dynamic buckling analysis by FEM, in which lumped masses on the shell side wall and initial imperfection, etc. can be taken into account are reported.

## 2. OUTLINE OF THE ANALYTICAL PROCEDURE

### 2.1 *Basic equations*

#### 2.1.1 *Analytical model*

As shown in Fig.1, a cylindrical coordinate $(r, \theta, Z)$ was applied here since an axisymmetric cylindrical shell was treated here.

#### 2.1.2 *Formulation for the structure*

The structure was defined by the region $\Omega_s$ with boundaries $\Gamma_N$, $\Gamma_D$ as shown in Fig.2. The governing equation for this structure will be,

$$\rho_s \frac{\partial^2 U_i}{\partial t^2} = \frac{\partial \sigma_{ij}}{\partial X_i} + b_i \quad in \ \Omega_s \tag{1}$$

where, $\rho_s$ means the density of the structure, $U_i$ is the displacement, $\sigma_{ij}$, $X_j$, $b_i$ are the stress, coordinate and the body force respectively. The boundary conditions at the wall will be given by the following equations,

$$\sigma_{ij} n_j |\Gamma_n = f_i \tag{2}$$

$$U_i \ |\Gamma_D = U_i^0 \tag{3}$$

where, $n_j$ is the outward unit normal vector and $f_i$ is the exciting force.

#### 2.1.3 *Stress and strain components*

The element coordinates are defined by $\zeta$, $\theta$, $\psi$, $\beta$

and $S$ as illustrated in Fig.3. The element displacements are $w$, $v$, $u$ for $\zeta$, $\theta$, $S$ respectively.

The stress will be expressed by the sum of the linear term and the nonlinear term, and furthermore the linear term will be given by the sum of the membrane and the bending strain. Thus,

$$\varepsilon = \varepsilon_L + \varepsilon_{NL}/2 \tag{4}$$

$$\varepsilon_L = \varepsilon_L^m + \zeta\chi_L^b \tag{5}$$

where the subscripts $L$, $NL$ mean the linear and the nonlinear term respectively. The superscripts $m$, $b$ mean the membrane and the bending component respectively. Each component for $\varepsilon_L^m$, $\chi_L^b$ and $\varepsilon_{NL}$ will be given by the Eqs.(6)~(8) as follows.

$$\varepsilon_L^m = \begin{Bmatrix} \varepsilon_s^L \\ \varepsilon_\theta^L \\ \gamma_{s\theta}^\Delta \end{Bmatrix} = \begin{Bmatrix} \partial u/\partial s \\ 1/r(w\cos\Psi + u\sin\Psi + \partial v/\partial\theta) \\ 1/r(r\partial v/\partial s + \partial u/\partial\theta - v\sin\Psi) \end{Bmatrix} \tag{6}$$

$$\chi_L^b = \begin{Bmatrix} \chi_s^L \\ \chi_\theta^L \\ \chi_{s\theta}^L \end{Bmatrix} = \begin{Bmatrix} \partial\beta/\partial s \\ 1/r^2(-\partial^2 w/\partial\theta^2 + r\beta\sin\Psi \\ +\partial v/\partial\theta\cos\Psi) \\ 2/r^2(r\partial\beta/\partial\theta + \partial w/\partial\theta\sin\Psi \\ +r\partial v/\partial s\cos\Psi - v\sin\Psi\cos\Psi \end{Bmatrix} \tag{7}$$

$$\varepsilon_{NL} = \begin{Bmatrix} \varepsilon_s^{NL} \\ \varepsilon_\theta^{NL} \\ \gamma_{s\theta}^{NL} \end{Bmatrix} = \begin{Bmatrix} (\partial u/\partial s)^2 + (\partial v/\partial s)^2 + (\partial w/\partial s)^2 \\ 1/r^2\left[(+\partial w/\partial\theta - v\cos\Psi)^2 \right. \\ +(\partial u/\partial\theta - v\sin\Psi)^2 \\ \left. +(w\cos\Psi + u\sin\Psi + \partial v/\partial\theta)^2\right] \\ 2/r\left[\partial w/\partial s(\partial w/\partial\theta - v\cos\Psi)\right. \\ +\partial u/\partial s(\partial u/\partial\theta - v\sin\Psi) \\ \left. +\partial v/\partial s(w\cos\Psi + u\sin\Psi + \partial v/\partial\theta)\right] \end{Bmatrix} \tag{8}$$

The out of plane shear strain $\varepsilon_K$ was defined by the Eq.(9).

$$\varepsilon_K = \partial w/\partial s + \beta \tag{9}$$

For the thin shell structures, $\varepsilon_K$ will approximately become zero. Therefore,

$$-\partial w/\partial s = \beta \tag{10}$$

In order to avoid the rocking phenomena, these elements will be evaluated by one point integration at the element center.

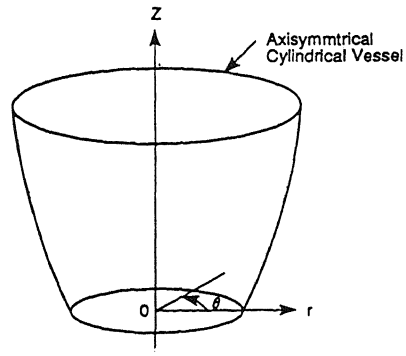


Fig.1 Analytical Model

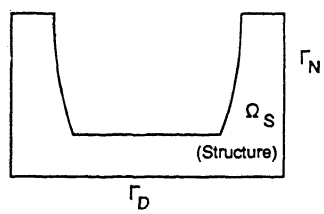


Fig.2 Region and Symbols

### 2.1.4 *Nodal displacement*

($u$, $v$, $w$, $\beta$) were developed in the following Fourier series after expressing by the linear equation in each element and employing the characteristics of the axisymmetric structure.

$$\begin{Bmatrix} u \\ v \\ w \\ \beta \end{Bmatrix} = \sum_{k=1}^{N} \begin{bmatrix} \cos k\theta & & & 0 \\ & \sin k\theta & & \\ & & \cos k\theta & \\ 0 & & & \cos k\theta \end{bmatrix} \begin{Bmatrix} u_k^s \\ v_k^s \\ w_k^s \\ \beta_k^s \end{Bmatrix} + \sum_{l=1}^{N} \begin{bmatrix} \sin l\theta & & & 0 \\ & \cos l\theta & & \\ & & \sin l\theta & \\ 0 & & & \sin l\theta \end{bmatrix} \begin{Bmatrix} u_k^a \\ v_k^a \\ w_k^a \\ \beta_k^a \end{Bmatrix} \tag{11}$$

### 2.1.5 *Initial imperfection*

In discussing the buckling problem of a cylindrical shell, the effect of the initial imperfection cannot be ignored. The nonlinear term in Eq.(6) can be expressed as the quadratic part of the displacement. Thus,

$$\varepsilon_{NL}(u) = \varepsilon_Q(u, u) \tag{12}$$

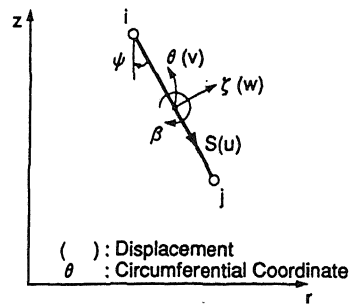


Fig.3 Element Coordinate and Displacement

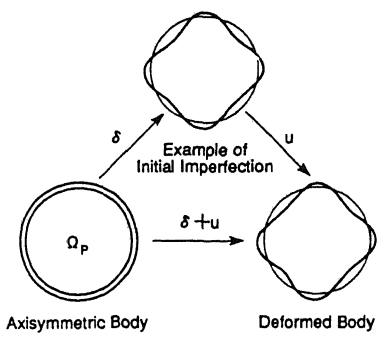


Fig.4 Definition of Displacement

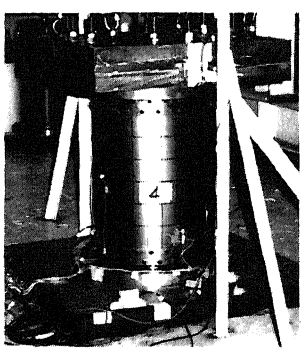

Fig.5 Test Speciman ($l$/R=2.4)

Defining the cylindrical coordinate $\Omega_p$ shown in Fig.4 and expressing the initial imperfection from the axisymmetric body by $\delta$ in a total Lagrange coordinate, the strain for the displacement $u$ will be given by the following equation. (Morihana, et al., 1980)

$$\varepsilon = \varepsilon_L(u) + \varepsilon_Q(\delta, u) + \varepsilon_Q(u, u)/2 \qquad (13)$$

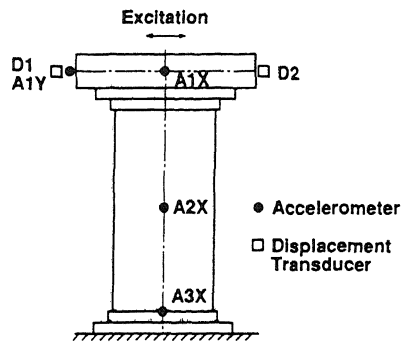


Fig.6 Measured Point

Table 1 Dimensions for Test Specimen

| No. | $R/t$ | $l/t$ | $R$ (mm) | $t$ (mm) | $l$ (mm) | material |
|---|---|---|---|---|---|---|
| 1 | 500 | 2.4 | 250 | 0.5 | 600 | steel |
| 2 | 500 | 1.5 | 250 | 0.5 | 375 | steel |

### 2.1.6 *Dynamic response analysis*

The equation of motion will become as follows from Eqs.(1)~(13).

$$[M_S]\{\ddot{U}\} + [C_S]\{\dot{U}\} + [K_S - K_G]\{U\} = \{f\} \qquad (14)$$

where $[M_S]$, $[C_S]$, $[K_S]$ are the mass matrix, damping matrix and the stiffness matrix of the structure respectively, and $\{f\}$ is the exciting force vector. $[K_G]$ is the geometric stiffness matrix given by the following equation.

$$[K_G] = [K(\sigma)] + [K(u)] \qquad (15)$$

When analyzing the Eq.(14) by direct integration method, the damping matrix $[C_S]$ can be given by Rayleigh damping, while in applying the modal analysis, modal damping will be needed.

## 2.2 *Buckling analysis*

Direct integration method will need huge CPU time since the stiffness matrix should be calculated for each time step because of the nonlinearity. Therefore, the modal analysis technique was applied here. Equation (15) will be evaluated using the displacements obtained from Eq.(14). Finally, the buckling analysis can be performed as an eigen value analysis.

$$([K_I] + \lambda[K_G])\{\Phi\} = 0 \qquad (16)$$

where, $[K_I]$ and $\{\Phi\}$ are the initial stiffness matrix and the buckling mode vector respectively. Buckling

will occur when the eigen value $\lambda$ will fall into the region as $0<\lambda<1$.

## 3. ANALYTICAL RESULTS

The analytical results were compared to the experimental results (Fujita, et al., 1990) and discussed. The test procedure will be stated briefly before going to the analytical results.

### 3.1 *Experiment*

Thin cylindrical shells made of steel were used as test specimens at the top of which a weight was attached for adjusting a 1st mode natural frequency as a beam structure as illustrated in Fig.5. These test specimens were installed on the 3-D large scale earthquake simulator and excited horizontally by EL Centro NS wave. Seismic responses such as acceleration and displacement at the top of the cylinder were measured at each excitation level which was increased step by step. The measured points and the dimensions for the test specimen were shown in Fig.6 and Table 1. The dimension of $l/R$ was varied as 2.4 and 1.5 under the constant $R/t$ ($R/t$=500, $R$=250mm, $t$=0.5mm).

### 3.2 *Analytical results*

#### 3.2.1 *Analytical model*

In this analysis, the top weight was also modeled as a thick axisymmetric element in order to improve the analytical accuracy. Before conducting the response analysis, the natural frequency and mode were analyzed. These results which are shown in Table 2 and Fig.7, are in good agreement with the experimental values, thus proving that the analytical model is appropriate.

#### 3.2.2 *Seismic response analysis*

The typical examples of the time history for the seismic response acceleration and displacement before buckling are shown in Figs.8. It was noted that the analytical time history was in very good agreement with the experimental one in a large amplitude region, therefore, we confirmed that the evaluation method proposed here will give a good estimation for the linear response.

#### 3.2.3 *Buckling analysis*

Buckling analysis was performed for two kinds of cylindrical shells shown in Table 1 and the deformation mode and the critical acceleration was obtained, where the circumferential wave numbers up to 20th were taken into account and the initial imperfection was ignored.

Table 2 1st Mode Natural Frequency (Hz)

| | Exp. | Cal. |
|---|---|---|
| No.1 | 14.4 | 14.7 |
| No.2 | 20.5 | 20.4 |

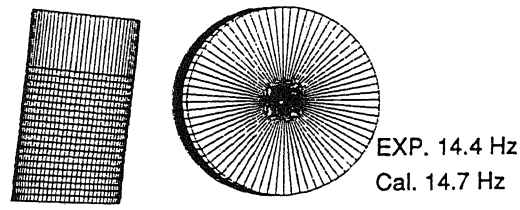


Fig.7 Analytical Result for Natural Frequency and Mode (No.1)

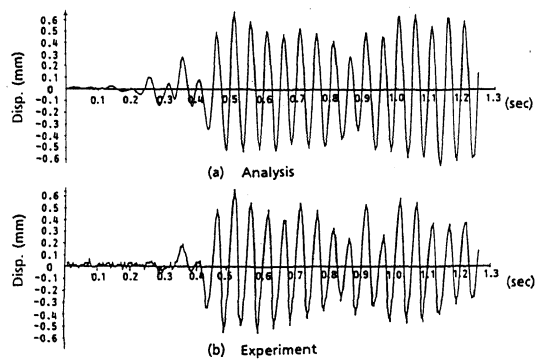


Fig.8 Analitycal Time History for Displacement (No.1)

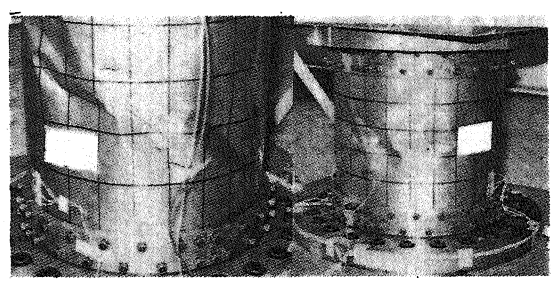

(a) No.1 Specimen ($l/R$=2.4) (b) No.2 Specimen ($l/R$=1.5)

Fig.9 Buckling Deformation Pattern by Experiment

From these results, the present dynamic buckling analysis method is known to be effective in predicting the critical acceleration and the buckling deformation of the cylindrical shell induced by the seismic excitation.

Figures 9 and 10 illustrate the buckling deformation pattern by the experiment and the analysis respectively. Buckling deformation was observed at around the middle

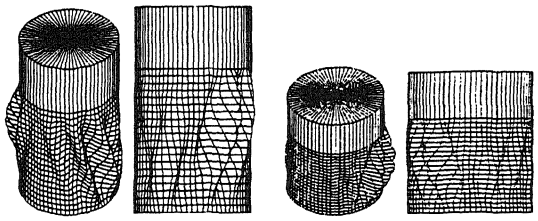

(a) No.1 Specimen (b) No.2 Specimen

Fig.10 Buckling Deformation Pattern by FEM

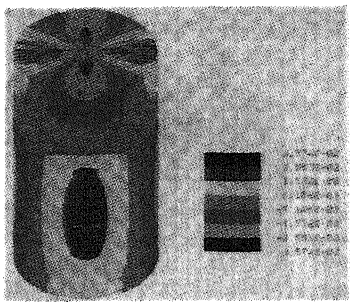

Fig.11 Stress Distribution by FEM (No.1)

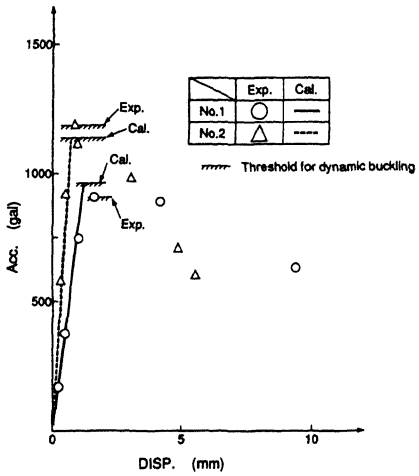


*Fig.12 Relationship between Acceleration and Displacement*

portion of the side wall and close to the perpendicular direction against the exciting direction of the cylindrical shell, revealing a so-called "Shear buckling deformation." These buckling deformations will be very hard to coincide with the experimental values, since in the experiment, the seismic excitation will continue for several seconds after the buckling occurs, then the occurrence and vanishment of the deformation will refrain for several times yielding to the irregular

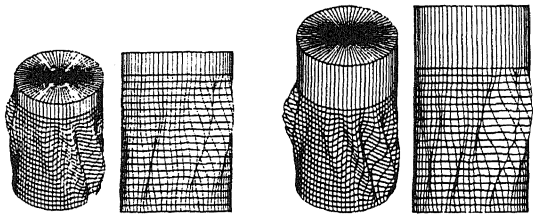

(a) R/t=300 (b) R/t=500

Fig.13 Deformation Patterns of R/t=300, 500

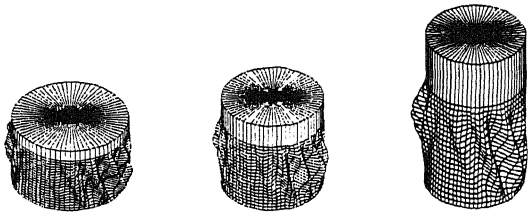

(a) $l$/R=1 (b) $l$/R=1.5 (c) $l$/R=2.4

Fig.14 Deformation Patterns for $l$/R=1.0, 1.5, 2.4

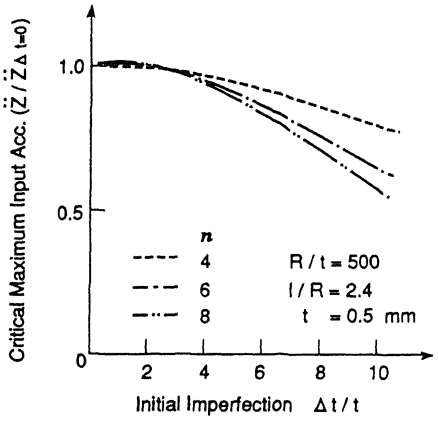


Fig.15 Initial Imperfection and Critical Input Acceleration

deformation pattern.

By taking these facts into consideration, the analytical values for the buckling deformation pattern and its location seem to be in good correspondence with the experimental values. The stress distribution at the side wall was also analyzed for the cylinder with $l/R$=2.4. The results are shown in Fig.11 and are in good consistency with the experimental deformation pattern shown in Fig. 9.

The relationship between the acceleration and the displacement at the cylinder top is also plotted in Fig.12. It was found that the acceleration is almost proportional to the displacement until buckling, but decreases after buckling, while the displacement will increase rapidly. The maximum input acceleration

obtained by the analysis at the buckling is thought to be in a good agreement with the experimental value.

### 3.2.4 *Buckling deformation and the cylinder dimension*

The influence of the dimensions of a cylindrical shell on the buckling deformation will be discussed here. The buckling deformation for the cylinder with $R/t$=300 and 500 was analyzed under constant $l/R$=2.4, i.e., the thickness $t$ was varied as 0.5mm and 0.83mm while the radius $R$ was kept constant. As shown in Fig.13, the number of the deformation wave tends to become less along with decreasing $R/t$. This corresponds to the inclination by the static buckling analysis against the twisting load, and shows that the present dynamic buckling analytical method is enough accurate.

On the other hand, the buckling deformations for the various $l/R$, i.e., $l/R$=1, 1.5 and 2.4 with constant $R/t$ ($R/t$=500) are illustrated in Fig.14. The number of the buckling deformation wave tends to larger against decreasing $l/R$.

### 3.2.5 *Initial imperfection and buckling threshold*

Influence of the initial imperfection on the dynamic buckling critical input acceleration and the buckling deformation was studied here using a cylinder with $R/t$=500 and $l/R$=2.4. The initial imperfection was applied as $\Delta t \cos n\theta$ and $\Delta t$ was varied within the range of $2 \leq \Delta t/t \leq 10$ for $n = 4, 6, 8$, where $t$ means the thickness of the cylinder.

The analytical results were plotted in Fig.15, where the vertical axis means the nondimensional critical maximum input acceleration $\ddot{Z}/\ddot{Z}\Delta t = 0$ and the horizontal axis shows the nondimensional initial imperfection $\Delta t/t$. It is known that the large initial imperfection will cause the decrease of critical buckling acceleration independently on the value of $n$, such as that the initial imperfection of 4 times of the thickness will give the 5% reduction in the critical buckling acceleration. And the reduction rate becomes large according to the increase of the circumferential wave number $n$. However, the critical buckling acceleration tends to become large slightly around $\Delta t/t$=1. This implies that the small initial imperfection will act toward the better side, but the further investigation will be needed to derive the conclusions.

The relationship between the initial imperfection and the buckling deformation was plotted for $n$=18 in Fig.16, and Fig.17 shows the influence of the circumferential wave number $n$.

It is known that the large initial imperfection will change the buckling deformation pattern, that is, the deformation will be concentrated in a small portion, moreover the different wave number $n$ will give the different deformation pattern.

The actual structure has more or less initial imperfections, therefore, the redundancy should be included to some extent in the structural design. And the quantitative value should be evaluated for each structure since the magnitude of the influence of the initial imperfection will depend on the dimensions of the cylindrical shell.

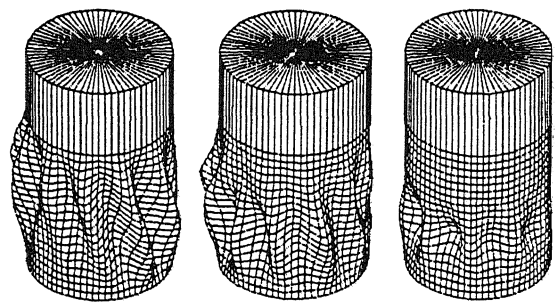

(a) Δt=0.5mm (b) Δt=3mm (c) Δt=5mm

Fig.16 Deformation Patterns for Various Initial Imperfections

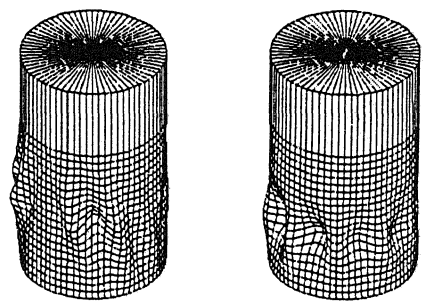

(a) n=4 (b) n=8

Fig.17 Deformation Patterns for n=4, 8

## 4. CONCLUSIONS

The evaluation method of dynamic buckling of a cylindrical shell due to random load such as wind or seismic load was developed and the validity was discussed by comparing the test results. And the influence of the initial imperfection on the critical buckling input acceleration was also investigated using this analytical method. The following items were obtained.

(1) The present evaluation method for dynamic buckling will have enough accuracy for estimating the natural frequency, the linear response characteristics, the critical buckling threshold and the buckling deformation pattern.

(2) This analytical method seems to be practical because this is based on the modal analysis and does not need so large CPU time.

(3) The larger the initial imperfection and the larger the wave number $n$, the smaller the critical buckling

input acceleration.

(4) The initial imperfection will change the buckling deformation pattern.

## REFERENCES


Yamaki, N. 1984. Dynamic instability and vibration of the liquid-filled cylindrical shell (in Japanese). Transactions of the JSME C 50, No.449: 3-10.

Tani, J. and Chiba, M. 1985. Experimental study on the dynamic stability of nuclear containment vessel under horizontal excitation. SMiRT 8th, K2016: 447-451.

Chiba, M., et al. 1988. Dynamic Stability of liquid filled cylindrical shells under periodic shearing force. ASME PVP 4: 241-253.

Combescure, A., et al. 1987. Dynamic behavior of liquid storage tanks. SMiRT 9th K14/1: 781-786.

Fujita, K., et al. 1990. Experimental study on the dynamic buckling of cylindrical shell due to seismic excitation. ASME PVP 191: 31-36.

Fujita, K., et al. 1990. Study on the dynamic buckling of cylindrical shell due to random excitation. Proceedings of JSME D: 195-197.

Fujita, K., et al. 1991. Experimental study on the dynamic buckling of a cylindrical shell due to seismic excitation. JSME International Journal 34, No.3: 339-344.

Morihana, et al. 1990. Research on general instability of cylindrical shells reinforced by ring stiffness under uniform pressure. Journal of the society of naval architects of Japan 168: 431-440.

Liu, W. K. and Uras, R. A. 1989. Transient buckling analysis of liquid-storage tanks-Part II: Applications. ASME PVP 157: 41-46.